Theory of the recombination of nonequilibrium carriers in type-II heterostructures

G. G. Zegrya and A. D. Andreev

A. F. Ioffe Physicotechnical Institute, Russian Academy of Sciences, 194021 St. Petersburg, Russia

A theory of the recombination of nonequilibrium carriers in type-II semiconductor heterostructures with quantum wells is devised for the first time. Analytical expressions for the radiative recombination and Auger recombination rates are obtained. It is shown that the Auger recombination mechanisms in type-I and type-II heterostructures differ fundamentally.
A fundamentally new result is obtained: the Auger recombination rate has a minimum at certain values of the heterostructure parameters. Such effective suppression of the Auger recombination processes in type-II heterostructures is associated with the short-range character of the Coulomb interaction of the electrons participating in the recombination process. It is also shown that the radiative recombination processes take place with equal efficiency in type-I and type-II heterostructures and that their rates are comparable. The possibility of regulating the Auger recombination rate in type-II heterostructures by varying the parameters of the structure is demonstrated. The effectiveness of using type-II heterostructures as opposed to type-I heterostructures to create optoelectronic devices is also demonstrated. © *1996 American Institute of Physics.* [S1063-7761(96)02002-X]

1. INTRODUCTION

Semiconductor quantum structures (single heterobarriers, quantum wells, superlattices, and quantum dots) have been actively investigated in recent years.[1] The interest in such structures from both the fundamental and practical standpoints is due to the occurrence of several phenomena in them which are not observed in homogeneous semiconductors.[2,3]

Semiconductor quantum structures may be of type I or type II.[4] In type-I heterostructures the offsets of the conduction band and the valence band at the interface between the two materials are in opposite directions (Fig. 1a). Type-II heterostructures have the following distinguishing features:[4] 1) the offsets of the conduction band (V_c) and the valence band (V_v) are in the same direction (Fig. 1b) and have different signs: $V_c > 0$, $V_v = -|V_v| < 0$; 2) in contrast to the case of type-I heterostructures, here the electrons and holes are spatially separated, so that recombination is possible only by means of tunneling through the heterobarrier.

As far as we know, the literature does not offer any material devoted to a theoretical investigation of Auger recombination processes in type-II heterostructures. As was previously shown in Ref. 3, the mechanisms of Auger recombination in heterostructures and in bulk semiconductors are essentially different. In heterostructures Auger recombination is a threshold-free process owing to the interaction of the carriers with the heterointerface, since there is no conservation law for the quasimomentum component perpendicular to the heterointerface; here the Auger recombination rate is a power function of the temperature. We recall that in a bulk semiconductor the Auger recombination rate is an exponential function of the temperature.[5] It will be shown below that in type-II heterostructures the Auger recombination rate is also a power function of the temperature, but the Auger re-

combination mechanisms in heterostructures of types I and II are fundamentally different.

The purpose of the present work is to theoretically investigate the recombination processes of nonequilibrium carriers in type-II heterostructures. We shall consider the radiative recombination and nonradiative Auger recombination processes in detail.

Type-II heterostructures have two important channels for Auger recombination: 1) an Auger process involving two electrons and one hole (the CHCC process); 2) an Auger process involving one electron and one hole with passage of a second hole into a spin-split-off band (the CHHS process). In the present work we restrict ourselves to consideration of the CHCC process (Fig. 2), since it dominates the CHHS process if $(E_g - \Delta_{SO})/E_g > m_c/m_{SO}$ holds where Δ_{so} is the spin-orbit splitting constant, E_g is the effective band gap width (see Fig. 2), and m_c and m_{SO} are the effective masses of an electron and an SO hole.

We note that in type-II heterostructures, unlike those of type I, the CHCC Auger process involves two channels (Fig. 2): 1) an electron tunnels through the heterobarrier and recombines with a hole in the quantum well (the E channel); 2) a hole tunnels through the heterobarrier and recombines with an electron in the quantum well (the H channel). The contributions of these two channels to the Auger recombination matrix element are of the same order owing to the interconversion of light and heavy holes when they interact with the heterointerface. It turns out that only the E channel is important in the radiative recombination process.

2. BASIC EQUATIONS

To calculate the radiative recombination rate R and the Auger recombination rate G it is first necessary to find the wave functions of the carriers in a type-II heterostructure. Figure 2 shows the band diagram of such a structure with

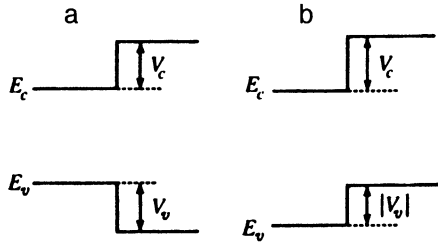FIG. 1. Band diagram of type-I (a) and type-II (b) heterostructures.

quantum wells. To the left of the point $x=0$ (in the region $x<0$) there is a quantum well of width a for electrons, and in the region $x>0$ there is a quantum well of width b for holes. We shall henceforth assume that nonequilibrium electrons and holes are trapped in these wells. We note that the effective band gap width E_g (i.e., the minimal energy separation between the electron and hole states) is smaller than the band gap widths for both semiconductors (see Fig. 2). As was previously noted,[3,5] the wave functions of the carriers must be calculated in a multiband approximation. It will be shown below that this is especially important for type-II heterostructures, since there are two channels for the recombination of electrons and holes (the E and H channels). These two channels interfere with one another owing to the interconversion of light and heavy holes. Therefore, the Auger recombination matrix element must be calculated with consideration of the complex structure of the valence band, particularly, the interconversion of light and heavy holes when they interact with the heterointerface.

We use the simplest multiband approximation, viz., the Kane model[6,7] with vanishingly small spin-orbit coupling. The influence of the spin-orbit coupling on the Auger recombination rate is discussed below. In this model the basis wave functions of the bottom of the conduction band and the top of the valence band are chosen in the form of $|s\rangle$ and $|p\rangle$ func-

tions (the x axis is perpendicular to the plane of the eterointerface). The wave functions of the electrons and holes are the result of superposition of the basis states:

$$\psi = u(\mathbf{r})|s\rangle + \mathbf{v}(\mathbf{r})|\mathbf{p}\rangle, \tag{1}$$

where $u(\mathbf{r})$ and $v(\mathbf{r})$ are the smooth envelopes of Bloch functions. The system of equations for the envelopes has the form[7]

$$\left[E - \frac{E_g}{2} - U_c(x)\right]u - \gamma\,\hat{\mathbf{k}}\cdot\mathbf{v} = 0,$$

$$\left[E + \frac{E_g}{2} - U_c(x) + \frac{\hbar^2\hat{\mathbf{k}}^2}{2m_h}\right]\mathbf{v} - \gamma\,\hat{\mathbf{k}}u = 0. \tag{2}$$

Here $\hat{\mathbf{k}} = -i\nabla$, γ is the Kane matrix element, which is identical for both semiconductors, and m_h is the effective mass of the heavy holes. The band offsets $U_c(x)$ and $U_v(x)$ are

$$U_c(x) = \begin{cases} 0, & -a<x<0, \\ V_c, & x<-a, \quad x>0, \end{cases}$$

$$U_v(x) = \begin{cases} 0, & 0<x<b, \\ V_c, & x>b, \quad x<0. \end{cases}$$

We note that V_c and V_v have different signs in type-II heterojunctions: $V_c>0$, $V_v=-|V_v|<0$. According to (2), the spectrum of the energy E is divided into an electron branch, a light hole branch, and a heavy hole branch.

The electron and hole wave functions determined from (2) must satisfy the following boundary conditions at the interfaces. The components u and v_x for the electrons are continuous at the heterointerfaces at $x=-a$, 0, b:[3]

$$u^> = u^<, \quad v_x^> = v_x^<. \tag{3}$$

Here the superscripts $<$ and $>$ on the components u and $\mathbf{v}$ refer to the values of these components to the left and to the right of the heterointerface, respectively. The components of the electron wave function parallel to the heterointerface v_y and v_z undergo a discontinuity. We note that in our model we neglected the term $\hbar^2\hat{\mathbf{k}}^2/(2m_h)$ in (2) when the electron wave functions were found, as well as when the boundary conditions (3) were derived.[3] Consideration of this term in the calculation of the electron wave functions is beyond the accuracy of the envelope-wave-function approximation. However, this term is of fundamental importance for the holes, since it leads to the interconversion of light and heavy holes when they interact with a heterointerface. The components v_x, v_y, and v_z, as well as the derivatives $\partial v_y/\partial x$ and $\partial v_z/\partial x$, are continuous at the heterointerfaces at $x=-a$, 0, and b. However, the derivative $\partial v_x/\partial x$ and u undergo a discontinuity:

$$\mathbf{v}^> = \mathbf{v}^<, \quad \frac{\partial v_y^>}{\partial x} = \frac{\partial v_y^<}{\partial x}, \quad \frac{\partial v_z^>}{\partial x} = \frac{\partial v_z^<}{\partial x},$$

$$\frac{\partial v_x^>}{\partial x} - \frac{\partial v_x^<}{\partial x} = i\gamma\frac{2m_h}{\hbar^2}(u^> - u^<). \tag{4}$$

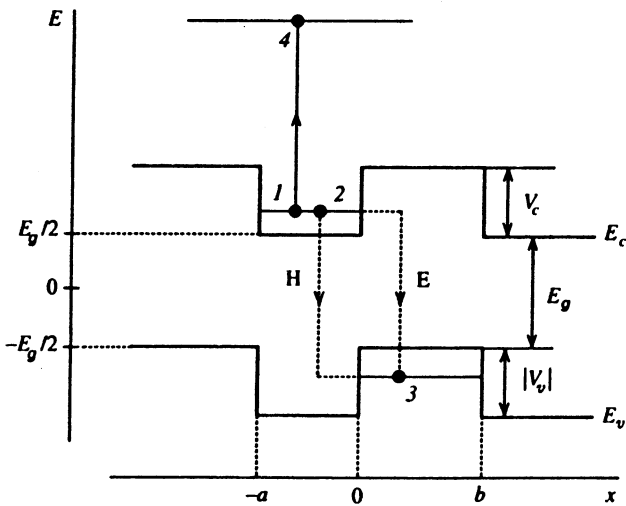The boundary conditions for the electron (3) and hole (4) wave functions were obtained from the system of Kane equa-

FIG. 2. Schematic representation of the band diagram of a type-II heterostructure with quantum wells: *1* and *2*-initial states of the particles; *3* and *4*-final states; H and E are two possible channels for the recombination of electron *2* and hole *3*.

tions (2) by integrating with respect to the transverse coordinate x and invoking the continuity of the x component of the flux density j_x.

As is well known,[8] the wave functions of particles (electrons and holes) in a symmetric quantum well are either even or odd functions of the coordinates. In the present paper we consider quantum wells which are not excessively narrow for the electrons and holes (rather than δ-function quantum wells): $\kappa_c b \gg 1$, $\kappa_l a \gg 1$, and $\kappa_h \gg 1$, where κ_c^{-1}, κ_l^l, and κ_h^{-1} are the characteristic damping distances of the wave function components near the barrier for electrons, light holes, and heavy holes, respectively. These inequalities are quite general and are valid for numerous semiconductor heterostructures.[4] In fact, using the characteristic values for heterobarriers V_c, $|V_v| \geqslant 0.1$ eV for wells of width a, $b \geqslant 80$ Å, we have $\kappa_c b \geqslant 3$ and $\kappa_l a \geqslant 3$. Therefore, the components of the envelope wave function u and v of the electrons and holes trapped in the quantum wells can also be classified according to their parity (even or odd). Below we shall present the wave functions of the carriers for states of a single parity.

The wave function of the electrons trapped in the region of the quantum well $(-a < x < 0)$ has the form

$$\psi_c(\mathbf{r}) = A \, \exp(i\mathbf{q} \cdot \boldsymbol{\rho}) \begin{pmatrix} \cos(kx_a) \\ i\lambda_- k \, \sin(kx_a) \\ \lambda_- q_y \, \cos(kx_a) \\ \lambda_- q_z \, \cos(kx_a) \end{pmatrix}. \tag{5}$$

Here $\mathbf{k} = (k_x, \mathbf{q}) \equiv (k, \mathbf{q})$ is the quasimomentum of an electron; $x_a = x + a/2$; $\lambda_- = \gamma/(E_c + |V_v| + E_g/2)$ is the characteristic wavelength, which corresponds to an electron energy of order E_g (when $\mathbf{k} = 0$ holds, we have $\lambda_- \approx \gamma/E_g \equiv \lambda_g = \hbar/\sqrt{2m_c E_g}$);

$$E_c = -\frac{|V_v|}{2} + \sqrt{\left(\frac{|V_v|}{2} + \frac{E_g}{2}\right)^2 + \gamma^2(k^2 + q^2)}$$

is the electron energy; ρ is the coordinate in the plane of the well; A is a normalization factor. For $x > 0$ (the subbarrier part) we have

$$\psi_c(\mathbf{r}) = B \, \exp(i\mathbf{q} \cdot \boldsymbol{\rho} - \kappa_c x) \begin{pmatrix} 1 \\ i\lambda_+ \kappa_c \\ \lambda_+ q_y \\ \lambda_+ q_z \end{pmatrix}, \tag{6}$$

where $B = A \cos(ka/2)$, $\lambda_+ = \gamma/[E_c + E_g/2]$, and κ_c^{-1} is the characteristic damping distance of the components of the electron wave function under the barrier:

$$\kappa_c^2 = q^2 + \frac{V_c - E_c + E_g/2}{\gamma \lambda_+}.$$

A similar expression holds for the subbarrier part of the wave function in the region $x < -a$. Using the boundary conditions (3), we obtain the dispersion equation for the even electron levels in the quantum well:

$$\tan \frac{ka}{2} = \frac{\kappa_c}{k} \frac{\lambda_+}{\lambda_-}. \tag{7}$$

Let us now consider the states of the light and heavy holes. In the region of the quantum well $(0 < x < b)$ the wave functions of the holes have the form

$$\psi_h(\mathbf{r}) = H \, \exp(i\mathbf{q} \cdot \boldsymbol{\rho}) \begin{pmatrix} 0 \\ iq \, \sin(p_h x_b) \\ -p_h(q_y/q)\cos(p_h x_b) \\ -p_h(q_z/q)\cos(p_h x_b) \end{pmatrix}$$

$$+ L \, \exp(i\mathbf{q} \cdot \boldsymbol{\rho}) \begin{pmatrix} A_w \cos(p_l x_b) \\ ip_l \, \sin(p_l x_b) \\ q_y \, \cos(p_l x_b) \\ q_z \, \cos(p_l x_b) \end{pmatrix}. \tag{8}$$

Here

$$A_w = \gamma^{-1} \left[E_h + \frac{E_g}{2} + \frac{\hbar^2}{2m_h} (q^2 + p_l^2) \right],$$

$q = \sqrt{q_y^2 + q_z^2}$, $x_b = x - b/2$, p_l and p_h are the x components of the wave vectors of the light and heavy holes, respectively, and L and H are the amplitudes of the wave functions corresponding to the light and heavy holes. Note that the amplitudes L and H should be calculated with consideration of interconversion of the light and heavy holes using the boundary conditions (4) (see Appendix A). The subbarrier part of the hole wave function in the region $x < 0$ has the form

$$\psi_h(\mathbf{r}) = \tilde{H} \, \exp(i\mathbf{q} \cdot \boldsymbol{\rho} + \kappa_h x) \begin{pmatrix} 0 \\ iq \\ \kappa_h(q_y/q) \\ \kappa_h(q_z/q) \end{pmatrix}$$

$$+ \tilde{L} \, \exp(i\mathbf{q} \cdot \boldsymbol{\rho} + \kappa_l x) \begin{pmatrix} -A_B \\ i\kappa_l \\ -q_y \\ -q_z \end{pmatrix}, \tag{9}$$

where

$$A_B = \gamma^{-1} \left[E_h + \frac{E_g}{2} + |V_v| + \frac{\hbar^2}{2m_h} (q^2 - \kappa_l^2) \right],$$

$\tilde{L}$ and $\tilde{H}$ are the amplitudes of the wave functions of the light and heavy holes with consideration of their interconversion in the subbarrier region (Appendix A). The hole wave function in the region $x > -b$ has a form similar to (9). We obtain the dispersion equation for the holes by plugging the expressions for the wave functions (8) and (9) into the boundary conditions (4):

$$\left(p_h \cot \frac{p_h b}{2} + \kappa_h \frac{E_h + E_g/2}{E_h + |V_v| + E_g/2} \right) \left(-p_l \tan \frac{p_l b}{2} \right.$$

$$\left. + \kappa_l \frac{E_h + E_g/2}{E_h + |V_v| + E_g/2} \right) = q^2 \left(\frac{|V_v|}{E_h + |V_v| + E_g/2} \right)^2. \tag{10}$$

For $q = 0$, Eq. (10) splits into two equations corresponding to noninteracting light and heavy holes. Figure 3 presents the spectrum of the holes as a function of q. For $q \neq 0$ interconversion of the light and heavy holes takes place. In the temperature range $T > E_{0h}$, where E_{0h} is the energy of the first size-quantization level of the heavy holes, the main contribution to the Auger recombination rate is made by values

G. G. Zegrya and A. D. Andreev   330

in the range $q > \pi/b$ (here and in the following the temperature T is measured in energy units). The influence of the spin-orbit coupling on the spectrum and wave functions of the holes can be neglected in this range of values of q (see Fig. 3). Therefore, as was pointed out above, the Kane model with vanishingly small spin-orbit coupling can be used to calculate the Auger recombination rate. An analysis reveals that the influence of the spin-orbit coupling on the Auger recombination process is confined to a quantitative change in the value of the recombination rate G. Thus, for $\Delta_{SO} \neq 0$ the Auger recombination rate acquires an additional factor $F(\alpha)$, where $\alpha = \Delta_{SO}/E_g$. For $\alpha = 0$ we have $F(\alpha) = 1$. It is significant that $F(\alpha)$ varies only slightly over the broad range of values $0 < \alpha < 10$: $1 < F(\alpha) < 2$. We also note that in the Kane model there are states of heavy holes polarized in the yz plane of the heterointerface in addition to the heavy hole states indicated above.[7] These states do not participate in the Auger recombination process, since the overlap integral of an electron with such holes is equal to zero.

The wave function of fast Auger electrons is a result of the superposition of the incident and reflected waves in the region $x < -a$ and the transmitted electron wave in the region $0 < x < b$:

$$\psi_4(\mathbf{r}) = A_4 \exp(i\mathbf{q} \cdot \boldsymbol{\rho})$$

$$\times \begin{pmatrix} \exp(i\bar{k}_4 x) + r \exp(-i\bar{k}_4 x) \\ \lambda_+ \bar{k}_4 [\exp(i\bar{k}_4 x) - r \exp(-i\bar{k}_4 x)] \\ \lambda_+ q_y [\exp(i\bar{k}_4 x) + r \exp(-i\bar{k}_4 x)] \\ \lambda_+ q_z [\exp(i\bar{k}_4 x) + r \exp(-i\bar{k}_4 x)] \end{pmatrix}, \quad (11)$$

$$\psi_4 = A_4 t \exp(i\mathbf{q} \cdot \boldsymbol{\rho} + i\bar{k}_4 x) \begin{pmatrix} 1 \\ \lambda_+ \bar{k}_4 \\ \lambda_+ q_y \\ \lambda_+ q_z \end{pmatrix}. \quad (12)$$

Here r and t are the amplitudes of electron reflection and transmission above the barrier; $\bar{k}_4$ is the x component of the quasimomentum of a fast Auger electron above the barrier, i.e.,

$$\bar{k}_4^2 + q_4^2 = \frac{E_4 - V_c - E_g/2}{E_4 + E_g/2} \lambda_+^{-2},$$

A_4 is a normalization factor,

$$A_4 = 1/\sqrt{1 + \lambda_+^2 (\bar{k}_4^2 + q_4^2)}.$$

The wave function in the region of the quantum well $(-a < x < 0)$ for the highly excited electrons has the form

$$\psi_4(\mathbf{r}) = A_4 \exp(i\mathbf{q} \cdot \boldsymbol{\rho})$$

$$\times \begin{pmatrix} d_+ \exp(ik_4 x) + d_- \exp(-ik_4 x) \\ \lambda_- k_4 [d_+ \exp(ik_4 x) - d_- \exp(-ik_4 x)] \\ \lambda_- q_y [d_+ \exp(ik_4 x) + d_- \exp(-ik_4 x)] \\ \lambda_- q_z [d_+ \exp(ik_4 x) + d_- \exp(-ik_4 x)] \end{pmatrix}. $$

$$(13)$$

Here d_- and d_+ are the amplitudes of the reflected and transmitted waves in the region of the quantum well, and k_4 is the
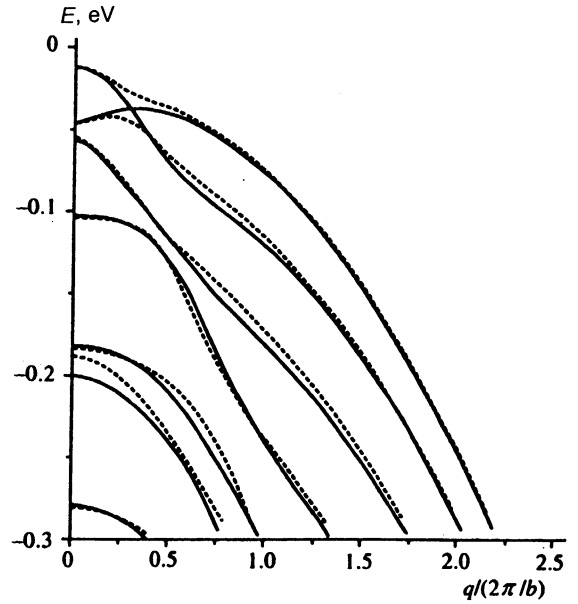

FIG. 3. Spectrum of holes in a type-II heterostructure as a function of the longitudinal momentum q. The solid lines represent the spectrum calculated from the dispersion equation (10). The dashed lines depict the anticrossings of the hole levels, which appear when the spin-orbit coupling is taken into account. The following parameters were taken for the calculation: $b = 80$ Å, $E_g = 0.96$ eV, $\Delta_{SO} = 0.6$ eV, $V_c = 0.15$ eV, $|V_v| = 0.4$ eV, $m_h = 0.4 m_0$, $m_c = 0.05 m_0$.

x component of the quasimomentum of the highly excited Auger electron in the region of the well, i.e.,

$$k_4^2 + q_4^2 = \frac{1}{\gamma^2} \left[E_4 - \frac{E_g}{2} \right] [E_4 + |V_v| + E_g/2].$$

The amplitudes r, d_+, and t are calculated using the boundary conditions (4) and the expressions for A_4 (Appendix A).

According to the standard rules of the theory of Auger processes,[3,5] the nonradiative Auger recombination rate is calculated using first-order perturbation theory with respect to the electron-electron interaction:

$$G = \frac{2\pi}{\hbar} \frac{1}{S} \sum_{1,2,3,4} |M|^2 \delta(E_1 + E_2 - E_3 - E_4)$$

$$\times f_c(E_1) f_c(E_2) f_h(E_3)[1 - f_c(E_4)], \quad (14)$$

where $f(E_i)$ is the distribution function of the ith particle $(i = 1,2,3,4)$ with respect to the energy, E_1 and E_2 are the energies of the initial states of the particles, E_3 and E_4 are the energies of the final states (we regard the hole state as the final state for one of the electrons participating in the process), S is the area of the heterojunction, M is the matrix element of the electron-electron interaction calculated with consideration of the antisymmetrization of the electronic wave functions of the initial and final states. The square of the absolute value of the matrix element after statistical averaging over the spin states of the initial electrons takes on the form

$$\langle |M|^2 \rangle = |M_I|^2 + |M_{II}|^2 - M_I M_{II}^*, \quad (15)$$

where

$$M_{\mathrm{I}}=\int \psi_2^*(\mathbf{r})\psi_3(\mathbf{r})\frac{e^2}{\kappa_0|\mathbf{r}-\mathbf{r}'|}\psi_1^*(\mathbf{r}')\psi_4(\mathbf{r}')d^3r\,d^3r'\,,$$

$$M_{\mathrm{II}}=\int \psi_1^*(\mathbf{r})\psi_3(\mathbf{r})\frac{e^2}{\kappa_0|\mathbf{r}-\mathbf{r}'|}\psi_2^*(\mathbf{r}')\psi_4(\mathbf{r}')d^3r\,d^3r'\,,$$

and κ_0 is the dielectric constant of the medium.

3. AUGER TRANSITION MATRIX ELEMENT

To calculate the matrix element we expand the Coulomb interaction potential in a Fourier integral. Then the matrix element of the electron-electron interaction takes the following form:

$$M_{\mathrm{I}}=\frac{4\pi e^2}{\kappa_0}\int \frac{d^3q}{(2\pi)^3}\frac{I_{14}(\mathbf{q})I_{23}(-\mathbf{q})}{q^2}, \tag{16}$$

where

$$I_{ij}(\mathbf{q})=\int d^3r\,\psi_i^*(\mathbf{r})\psi_j(\mathbf{r})e^{i\mathbf{q}\cdot\mathbf{r}}. \tag{17}$$

The expression for M_{II} is obtained from (16) by performing the corresponding interchange of indices $1\leftrightarrow2$. To calculate the matrix element we express the integrand in I_{14} in terms of the flux density. From the general form of the Kane equations we can obtain the scalar product $\psi_i^*\psi_j$ of two electron wave functions having the form of columns containing four components of the envelopes u and $\mathbf{v}$ [see (1)]:

$$\psi_i^*\psi_j=u_i^*u_j+\mathbf{v}_i^*\cdot\mathbf{v}_j=\frac{1}{E_i-E_j}\,\mathrm{div}\,\mathbf{j}_{ij}, \tag{18}$$

where

$$\mathbf{j}_{ij}=i\gamma(u_i^*\mathbf{v}_j+u_j\mathbf{v}_i^*). \tag{19}$$

Substituting (18) and (19) into (17) and performing the integration in the plane of the quantum well, we obtain the following expression for I_{14}:

$$I_{14}=\frac{\gamma}{E_4-E_1}\{(\mathbf{q}_4-\mathbf{q}_1)I_\parallel-qI_x\}\delta_{\mathbf{q}_\parallel+\mathbf{q}_4-\mathbf{q}_1,0}$$

$$\equiv \tilde{I}_{14}(q)\delta_{\mathbf{q}_\parallel+\mathbf{q}_4-\mathbf{q}_1,0}, \tag{20}$$

where

$$\mathbf{I}_\parallel=\int_{-\infty}^{\infty}e^{iqx}(u_4\mathbf{v}_{1\parallel}^*+u_1^*\mathbf{v}_{4\parallel})dx, \tag{21}$$

$$I_x=\int_{-\infty}^{\infty}e^{iqx}(u_4v_{1x}^*+u_1^*v_{4x})dx. \tag{22}$$

Here we took into account that $\mathbf{v}=(v_x,\mathbf{v}_\parallel)$, and $\delta_{\mathbf{q},0}$ is the Kronecker delta. We substitute the expression (20) for I_{14} into (16). As a result, with consideration of the explicit form of I_{23}, for the matrix element we obtain

$$M_{\mathrm{I}}=\frac{4\pi e^2}{\kappa_0}\int dx\,\psi_3(x)\psi_2^*(x)\int\frac{dq}{2\pi}\frac{e^{-iqx}\tilde{I}_{14}(q)}{(\mathbf{q}_1-\mathbf{q}_4)^2+q^2}$$

$$\times\,\delta_{\mathbf{q}_1+\mathbf{q}_2,\mathbf{q}_3+\mathbf{q}_4}\equiv \tilde{M}_{\mathrm{I}}\delta_{\mathbf{q}_1+\mathbf{q}_2,q_3+q_4}. \tag{23}$$

The matrix element M_{I} can be calculated exactly by analytical methods. It is convenient to use the following scheme to calculate it. We first calculate I_x and $I_\parallel$ (see Appendix B). Then we integrate with respect to q in (23) using the residue theorem.[9] It follows from (23) and (B1) that there are then two kinds of poles in the complex plane of q: 1) poles which correspond to a small momentum transfer $q=\pm i|\mathbf{q}_1-\mathbf{q}_4| \sim 1/\lambda_T$ during the Coulomb interaction, where $\lambda_T = \sqrt{\hbar^2/2m_hT}$; 2) poles which correspond to a large momentum transfer $q\approx Q$, where $Q\simeq 1/\sqrt{2}\lambda_g$ and $\lambda_g\ll\lambda_T$. We recall that the longitudinal momenta $\mathbf{q}_1$ and $\mathbf{q}_4$ of the particles are of the order of the thermal momenta; therefore, $|\mathbf{q}_1|,|\mathbf{q}_4|\ll Q$. As a result, the Auger transition matrix element separates into two parts:

$$M=M^{(1)}+M^{(2)}\equiv(\tilde{M}^{(1)}+\tilde{M}^{(2)})\delta_{\mathbf{q}_1+\mathbf{q}_2,\mathbf{q}_3+\mathbf{q}_4}, \tag{24}$$

where $M^{(1)}$ and $M^{(2)}$ are the contributions to the matrix element corresponding to small and large momentum transfers.

The following remarks are in order here. In homogeneous semiconductors the Coulomb interaction matrix element for Auger recombination contains only the part which corresponds to large momentum transfers due to the requirements of the energy and momentum conservation laws. The consequences of this are as follows:

1) the very indirect course of the transition of an electron from the initial to the highly excited final state in $\mathbf{k}$ space;

2) the threshold (exponential) dependence of the Auger recombination rate on the temperature.

As was previously shown by one of us,[3] in type-I semiconductor heterostructures the main contribution to the Coulomb interaction matrix element is made by the long-range part, which corresponds to small momentum transfers. This feature of the behavior of the Auger transition matrix element in the presence of a heterointerface is fundamentally related to the interaction of the carriers with the heterointerface. One result of such an interaction is the absence of a conservation law for the transverse (x) component of the quasimomentum of the particles. The consequences of this are as follows:

1) the threshold-free character of the Auger recombination process in quantum structures, where the rate is a power function of the temperature, rather than an exponential function, as in a homogeneous semiconductor;

2) the resonant character of the Auger transition, i.e., the transition of the electron from the initial state to the highly excited state takes place as a result of the transfer only of energy from the recombining electron-hole pair without momentum transfer; the electron obtains the momentum needed for the transition to the highly excited final state from the interaction with the heterointerface.

In type-II heterostructures, along with the long-range part of the Coulomb interaction matrix element, which corresponds to small momentum transfers, the short-range part, which corresponds to large momentum transfers, must be taken into account. Since the electrons and holes in type-II heterostructures are spatially separated, there are two channels for Auger recombination, viz., E and H (Fig. 2). As will be shown below, these two channels interfere with one another, causing a decrease in the matrix element $M^{(1)}$. In ad-

dition, $M^{(1)}$ is significantly smaller than $M^{(2)}$ when a certain relationship exists between V_c and V_v [see (31)]. Thus, in type-II heterostructures contributions to the Auger recombination rate are made by both the long-range part of the Coulomb interaction (small momentum transfers) and the short-range part of the Coulomb interaction (large momentum transfers).

In calculating $M^{(1)}$ and $M^{(2)}$ below, we shall use the following relationships between the parameters: $T \ll (V_c, |V_v|) \ll E_g$. Such a relationship between the parameters is observed for most semiconductor heterostructures. It is then convenient to calculate $M^{(1)}$ and $M^{(2)}$ separately.

3.1. Small momentum transfers

Let us proceed to the calculation of $M^{(1)}$. We consider the electron overlap integral $I_{14}(q)$ at small q. We expand I_{14} in powers of $1/Q$. Then, according to (20)–(22) and (B1), we obtain

$$\tilde{I}_{14} \simeq -\frac{\gamma q}{E_g} I_x, \tag{25}$$

$$I_x \simeq -\frac{i\gamma}{4E_g^2}(3V_c-|V_v|)[u_1(0)u_4(0)-e^{-iqa}u_1(-a)u_4(-a)]$$

$$+\frac{\kappa_c(3V_c-|V_v|)}{2Q^2E_g}[u_1(0)v_{x4}(0)+e^{-iqa}u_1(-a)v_{x4}(-a)]$$

$$+\frac{iq(5V_c-|V_v|)}{2Q^2E_g}[u_1(0)v_{x4}(0)-e^{-iqa}u_1(-a)v_{x4}(-a)]. \tag{26}$$

Here $q = \pm i|\mathbf{q}_1-\mathbf{q}_4|$, $u_1(0)$, $v_{x4}(0)$, and $u_4(0)$ are the values of the components of the envelope wave function at the hetero-interface $x=0$; $u_1(-a)$, $v_{x4}(-a)$, and $u_4(-a)$ are the values of the components at $x = -a$. We recall that the components u and v_x for electrons are continuous. Using the explicit expressions for I_x and $\mathbf{I}_{\parallel}$ (see Appendix B), we find that $|I_{\parallel}|/I_x \approx \sqrt{TV_c/E_g^2} \ll 1$; therefore, we have neglected $\mathbf{I}_{\parallel}$ in (25). In addition, in (25) we have taken into account that $E_4-E_1 \simeq E_g$.

To calculate I_x according to (22), we divide the integration with respect to x into three regions: the region of the well $(-a<x<0)$ and the two barrier regions $(x>0$ and $x<-a)$. It turns out that the contributions to the matrix element from the region of the quantum well and from the two barrier regions are of the same order, but of different sign. As a result, they cancel one another, so that a small parameter of order $\sqrt{V/E_g}$ [where V is a combination of V_c and $|V_v|$, see (26)] appears in the expression for I_x. Thus, the leading (with respect to $1/Q$) term in I_x is proportional to $1/Q^3$. In (26) we retained the next order in $1/Q$, i.e., $1/Q^4$, since the main term, which is proportional to $1/Q^3$, has the multiplier $3V_c-|V_v|$, which can be close to zero. It should be stressed that such a situation does not arise in type-I heterostructures, and it is sufficient to restrict the calculation of I_x to the main term, which is proportional to $1/Q^3$. In type-I heterostructures the main term in $1/Q$ is proportional to $(3V_c+V_v)/E_g$, where $V_v>0$.

We substitute the expression for $\tilde{I}_{14}$ [Eqs. (25) and (26)] into (23). Performing the integration with respect to q, we obtain

$$\tilde{M}_I = \frac{4\pi e^2}{\kappa_0} \int_{-\infty}^{+\infty} \psi_2^*(x)\psi_3(x)J(x)dx, \tag{27}$$

$$J(x) = \frac{\gamma^2}{8E_g^2}u_1^*(0)u_4(0)\exp(-p_{14}|x|)\Bigg\{(3V_c-|V_v|)\Bigg(1$$

$$+i\frac{\kappa_c}{Q}\Bigg)\text{sign }x+i(5V_c-|V_v|)\frac{p_{14}}{Q}\Bigg\}, \tag{28}$$

where $p_{14}=|\mathbf{q}_1-\mathbf{q}_4|\sim 1/\lambda_T$. We note that in (28) we neglected the terms which are proportional to $\exp(-p_{14}a) \ll 1$. This is correct when $p_{14}a \approx \sqrt{2m_hTa^2/\hbar^2} \simeq \sqrt{T\pi^2/E_{0h}} \gg 1$. Here and in the following we assume that $E_{0h}<T \ll |V_v|$.

Performing the integration with respect to x in (27), we obtain the final expression for the matrix element $M^{(1)}$ at small momentum transfers. Expressing the product $\psi_2^*(x)\psi_3(x)$ in (27) in terms of the flux density [see Eqs. (18) and (19)] and integrating in parts, we obtain

$$\tilde{M}_I^{(1)} = \frac{4\pi e^2}{\kappa_0}\frac{i\gamma^2}{8E_g^2}\frac{u_1(0)u_4(0)}{p_{14}}\Bigg\{(3V_c-|V_v|)\Bigg(1+i\frac{\kappa_1}{Q}\Bigg)$$

$$\times[J_h+J_e-2p_{14}u_2^*(0)v_{3x}(0)]+i(5V_c-|V_v|)$$

$$\times\frac{p_{14}}{Q}[J_h-J_e+2i(\mathbf{q}_3-\mathbf{q}_2)u_2^*(0)\mathbf{v}_{3\parallel}(0)]\Bigg\}, \tag{29}$$

where

$$J_e = \int_{-\infty}^{0}\Bigg\{p_{14}^2[u_2^*v_{3x}+u_3v_{2x}^*]$$

$$+i(\mathbf{q}_3-\mathbf{q}_2)\cdot\frac{\partial}{\partial x}(u_2^*\mathbf{v}_{3\parallel}+u_3\mathbf{v}_{2\parallel}^*)\Bigg\}dx, \tag{30}$$

where J_h is the same as J_e, except that it is taken in the range from 0 to ∞.

When M is calculated, it is important to take into account the interconversion of the light and heavy holes accompanying the interaction with the heterointerface. The matrix element M consists of two parts: the contribution from the region $x<0$ and the contribution from the region $x>0$. These two contributions correspond to two channels for the recombination of spatially separated electrons and holes (the E and H channels, see Fig. 2). The E channel corresponds to the recombination of an electron tunneling through the heterobarrier with holes, which transform into one another when they are reflected from the heterointerface. In the case of the H channel, an electron trapped in the well recombines with holes, which transform into one another when they tunnel through the heterobarrier. For quantum wells in which the size-quantization energy of the electrons and holes is much smaller than the height of the heterobarriers $(E_{0c} \ll V_c, E_{0h} \ll |V_v|)$, we find that the contributions of the E and H channels to $M^{(1)}$ are of the same order, but of different sign. Thus, there is destructive interference between these two channels for Auger recombination. Such interference produces an additional small parameter of order

$[T m_h / V_c m_c]^{3/2} < 1$ in the matrix element $M^{(1)}$ for type-II heterostructures in comparison with the Auger recombination matrix element for type-I heterostructures.[3,10] As a result, the Auger recombination matrix element for small momentum transfers equals

$$\tilde{M}_1^{(1)} = \frac{4\pi e^2}{\kappa_0} \frac{\gamma^3}{8 E_g^4} u_1^*(0) u_2(0) u_4(0) H \varepsilon_h \sin \frac{p_h b}{2}$$

$$\times \left\{ (3 V_c - |V_v|) \left(1 + \frac{i \kappa_1}{Q} \right) \left[\frac{m_h}{m_c} \frac{\mathbf{q}_3 \cdot (\mathbf{q}_3 - \mathbf{q}_2)}{q_3 V_e} \right. \right.$$

$$\left. + 2 \frac{q_3}{|p_l|} \sqrt{\frac{2 m_c}{|V_v| \hbar^2}} \right] + i \frac{p_{14}}{Q} (5 V_c$$

$$\left. - |V_v|) \frac{m_h}{m_c} \frac{\mathbf{q}_3 \cdot (\mathbf{q}_3 - \mathbf{q}_2)}{q_3 V_c} \right\}. \tag{31}$$

Here $\varepsilon_h = \hbar^2 (p_h^2 + q_3^2) / 2 m_h$ is the energy of a heavy hole measured from the valence-band edge of the semiconductor in the region of the quantum well $0 < x < b$;

$$u_1(0) = u_2(0) = A \cos \frac{ka}{2}, \quad u_4(0) = A_4 t.$$

Let us proceed to the calculation of $M^{(2)}$.

3.2. Large momentum transfers

In type-I semiconductor heterostructures the contribution to the Auger transition matrix element $M^{(2)}$ from large momentum transfers is small in comparison with the contribution from small momentum transfers:

$$\frac{M^{(2)}}{M^{(1)}} \sim \frac{T}{V_c} \sqrt{\frac{m_h}{m_c}} \ll 1.$$

As will be shown below, in type-II heterostructures this is not so: $M^{(1)}$ and $M^{(2)}$ can be of the same order, and under certain conditions the contribution $M^{(2)}$ from large momentum transfers can significantly exceed $M^{(1)}$. This difference between the mechanisms of Auger recombination in heterostructures of types I and II is attributed to the magnitude of the overlap integral I_{14} of the electrons in the initial state 1 and the final state 4 at small momentum transfers.

Using the expression (23) for M_1, we represent $\tilde{M}_1^{(2)}$ in the form

$$\tilde{M}_1^{(2)} = \frac{4\pi e^2}{\kappa_0} \left[\int_{-\infty}^{0} \psi_2^*(x) \psi_3(x) J_{14}^{(e)} dx \right.$$

$$\left. + \int_{0}^{\infty} \psi_2^*(x) \psi_3(x) J_{14}^{(h)} dx \right], \tag{32}$$

where

$$J_{14}^{(h)} = \int_0^\infty \frac{dq}{2\pi} I_{14}(q) \frac{e^{-iqx}}{q^2 + p_{14}^2}, \tag{33}$$

$J_{14}^{(e)}$ is the same as $J_{14}^{(h)}$, except that it is taken in the range from $-\infty$ to 0. When $J_{14}^{(e)}$ and $J_{14}^{(h)}$ are calculated using the residue theorem, only the poles corresponding to large momentum transfers $|q| \approx Q$ should be taken into account, and

the pole $q = \pm i p_{14}$ should be disregarded, since it was already taken into account in $M^{(1)}$. Performing the integration in (33) with respect to q, we obtain

$$J_{14}^{(h)} = \frac{B A_4 t}{(\bar{k}_4 + i \kappa_c)^2 + p_{14}^2} [1 + \gamma^2 \lambda_-^{(1)} \lambda_-^{(4)} (\mathbf{q}_1 \cdot \mathbf{q}_4$$

$$- i \kappa_c \bar{k}_4)] \exp(i x \bar{k}_4 - \kappa_c x). \tag{34}$$

Here $\lambda_-^{(i)} = \gamma / (E_i + |V_v| + E_g / 2)$, where $i = 1,4$. The expression for $J_{14}^{(e)}$ is presented in Appendix C. We substitute (34) and (C2) into (32). The integration with respect to x must be performed next. The integral with respect to x has the following form

$$\int_0^\infty f(x) e^{i\xi x} dx = -\frac{1}{i\xi} f(+0) + \frac{1}{(i\xi)^2} f'(+0)$$

$$- \frac{1}{(i\xi)^3} f''(+0) + \cdots. \tag{35}$$

A relation similar to (35) holds in the case of integration from $-\infty$ to 0. The expression (35) is obtained using integration by parts. Here we use $f(\pm\infty) = 0$ and note that $f(+0)$ is the value of f at the point $x = +0$. In our case $\xi \approx Q$ holds; therefore, Eq. (35) is nothing more than an expansion of $M^{(2)}$ in powers of $1/Q$. As in the case of small momentum transfers, we restrict ourselves to the first two nonvanishing terms in the expansion in powers of $1/Q$ in $M^{(2)}$. As a result, the integral with respect to x (from $-\infty$ to $+\infty$) equals

$$\int_{-\infty}^{\infty} f(x) e^{i\xi x} dx = -\frac{1}{i\xi} [f(+0) - f(-0)]$$

$$+ \frac{1}{(i\xi)^2} [f'(+0) - f'(-0)]$$

$$- \frac{1}{(i\xi)^3} [f''(+0) - f''(-0)] + ..., \tag{36}$$

where $f(-0)$ is the value of the function f at the point $x = -0$. It was assumed in (35) and (36) that $f(x)$ is a smooth function separately in $[-\infty, 0]$ and $[0, +\infty]$; both the function $f(x) \equiv u_2^*(x) u_3(x) + \mathbf{v}_2^*(x) \cdot \mathbf{v}_3(x)$ and its derivatives $f'(x), f''(x), ...$ have finite discontinuities at the heterointerface. The jumps in the function and its derivatives are calculated directly using the Kane equations (2) and the boundary conditions (4). As a result, for $\tilde{M}_1^{(2)}$ we obtain

$$\tilde{M}_1^{(2)} = \frac{4\pi c^2}{\kappa_0} u_1(0) u_2(0) u_4(0) \frac{1}{i \gamma Q^4} \left\{ (V_c - |V_v|) \right.$$

$$+ v_{3x}(0) + \varepsilon_h H \sin\left(\frac{p_h b}{2}\right) \frac{1}{Q} \left[\frac{m_h}{m_c} \frac{\mathbf{q}_2 \cdot \mathbf{q}_3}{q_3} \right.$$

$$\times \sqrt{\frac{2 m_h |V_v|}{\hbar^2}} + \frac{2 m_c}{\hbar^2} (V_c^{3/2} |V_v|^{-1/2}$$

$$\left. + |V_v|^{1/2} V_c^{1/2} + 2 |V_v| - 8 V_c) \right] \right\}. \tag{37}$$

G. G. Zegrya and A. D. Andreev   334

Here $v_{3x}(0)$ is the value of the component of the hole wave function at the heterointerface $x=0$. In the approximation $\epsilon_h \ll |V_v|$ for states of the parity for which v_{3x} is odd we have

$$v_{3x}(0) = iH \sin\left(\frac{p_h b}{2}\right)\left[\frac{q_3}{|p_l|}\sqrt{\frac{2m_c\varepsilon_h^2}{\hbar^2|V_v|}}\right.$$
$$\left. + \frac{\varepsilon_h}{|V_v|}\,q_3\left(1 + \frac{2m_c\varepsilon_h}{\hbar^2|p_l|^2}\right)\right]. \tag{38}$$

The expressions (24), (31), and (37) completely specify the Auger transition matrix element $M_{\rm I}$. As we have already noted above, $M_{\rm II}$ is obtained from $M_{\rm I}$ by means of the interchange of indices $1 \leftrightarrow 2$.

It follows from the expressions which we obtained for $M^{(1)}$ and $M^{(2)}$ that in type-II heterostructures the relationship between $M^{(1)}$ and $M^{(2)}$ greatly depends on the parameters of the heterostructure, viz., the heights of the heterobarriers V_c and V_v and the widths of the quantum wells for electrons (a) and holes (b) (Fig. 2). The following cases are possible, depending on the relationship between V_c and V_v: $M^{(1)} \gg M^{(2)}$; $M^{(1)} \sim M^{(2)}$; $M^{(1)} \ll M^{(2)}$.

4. AUGER RECOMBINATION RATE

To calculate the rate G, the square of the absolute value of the matrix element $|M|^2$ [see (15)] must be substituted into the expression (14), and the summation must be carried out over the initial and final states of the particles. We shall assume below that only the ground-state of the electron size-quantization is filled. As for the heavy holes, it was noted above that $T > E_{0h}$; therefore, we replace the summation over the hole size-quantization levels by integration with respect to p_h. Integration should also be performed over the states of the highly excited electron. Then for G we have

$$G = \frac{2\pi}{\hbar}\int\frac{d^2q_1}{(2\pi)^2}\int\frac{d^2q_2}{(2\pi)^2}\int\frac{d^2q_3}{(2\pi)^2}$$
$$\times \int\frac{dp_h}{2\pi}\int\frac{dk_4}{2\pi}\{|\tilde{M}_{\rm I}|^2 + |\tilde{M}_{\rm II}|^2 - \tilde{M}_{\rm I}\tilde{M}_{\rm II}^*\}\delta(E_1$$
$$+ E_2 - E_3 - E_4)f_c(E_1)f_c(E_2)f_h(E_3). \tag{39}$$

In deriving (39) we sum over $\mathbf{q}_4$ using the Kronecker delta corresponding to the conservation law for the longitudinal component of the momentum $\mathbf{q}$ [see (23)]. Then in (39) we perform the integration with respect to the momentum k_4 of the highly excited electron using the energy δ function. We use the explicit expressions for the energies of the electrons and holes, in which it is important to take into account the nonparabolic character of the spectrum of the highly excited electron, to represent the argument of the δ-function in the form

$$E_1 + E_2 - E_3 - E_4 \simeq \frac{3}{2}E_g - \sqrt{\frac{E_g^2}{4} + \gamma^2 k_4^2}. \tag{40}$$

In (40) we took into account that $|\mathbf{k}_1| \simeq |\mathbf{k}_2| \simeq \sqrt{m_c/m_h}|\mathbf{k}_3| \ll |\mathbf{k}_4|$. As a result, the integration with respect to k_4 gives

$$G = \frac{3}{\sqrt{2}\hbar\gamma}\int\frac{d^2q_1}{(2\pi)^2}\int\frac{d^2q_2}{(2\pi)^2}\int\frac{d^2q_3}{(2\pi)^2}$$
$$\times \int\frac{dp_h}{2\pi}\,(|\tilde{M}_{\rm I}|^2 + |\tilde{M}_{\rm II}|^2 - \tilde{M}_{\rm I}\tilde{M}_{\rm II}^*)_{E_4 = 3E_g/2}$$
$$\times f_c(E_1)f_c(E_2)f_h(E_3). \tag{41}$$

We perform the ensuing integration with respect to q_1, q_2, and q_3 using a polar coordinate system. The calculation of the integrals is a simple, but lengthy procedure. As we have already noted above, the heavy holes polarized in the plane of the heterointerface do not make a contribution to the Auger recombination rate. Therefore, in the expression for the rate we must require that the concentration of holes which participate in the recombination process be equal to half of the total concentration of holes. As a result, the final expression for the Auger recombination rate has the following form:

$$G = \tilde{G}\left(g_1 + \frac{V_c}{E_g}g_2 + \frac{T}{E_g}g_3\right) \equiv G_1 + G_2 + G_3. \tag{42}$$

Here

$$\tilde{G} = 32\sqrt{2}\pi^2\frac{E_B}{\hbar}\frac{T}{E_g}\frac{m_c}{m_h}n^2p\lambda_g^4\frac{\kappa_c^4\lambda_g^5}{b}\frac{\cos^4(ka/2)}{(1+\kappa_c a)^2}, \tag{43}$$

$$g_1 = \frac{(2V_c - |V_v|)^2}{|V_v|V_c} + \sqrt{\pi}\left(\frac{m_h}{m_c}\right)^{3/2}\left(\frac{T}{|V_v|}\right)^{1/2}\frac{3V_c - |V_v|}{4V_c}$$
$$\times\frac{2V_c - |V_v|}{V_c} + \left(\frac{m_h}{m_c}\right)^3\frac{T}{V_c}\left(\frac{3V_c - |V_v|}{4V_c}\right)^2, \tag{44}$$

$$g_2 = \frac{(3V_c - |V_v|)^2}{16V_c^2}\left[\frac{2V_c}{|V_v|} + \left(\frac{m_h}{m_c}\right)^{3/2}\left(\frac{\pi T}{|V_v|}\right)^{1/2} + \left(\frac{m_h}{m_c}\right)^3\frac{T}{2V_c}\right]$$
$$+ \left(\frac{m_h}{m_c}\right)^2\frac{T}{8V_c^3}(3V_c - |V_v|)(5V_c - |V_v|)\left[\left(\frac{V_c}{|V_v|}\right)^{1/2}\right.$$
$$+ \frac{3}{8}\left(\frac{m_h}{m_c}\right)^{3/2}\left(\frac{T}{V_c}\right)^{1/2}\right] + \frac{1}{16}\left(\frac{m_h}{m_c}\right)^4\left(\frac{T}{V_c}\right)^2\left(\frac{5V_c - |V_v|}{V_c}\right)^2, \tag{45}$$

$$g_3 = \frac{1}{8}\left(\frac{m_h}{m_c}\right)^2\left[\left(\sqrt{\frac{m_h}{m_c}\frac{|V_v|}{V_c}} + \frac{3V_c - |V_v|}{2V_c}\right)^2\right.$$
$$+ \frac{5V_c - |V_v|}{2V_c}\left(\frac{\pi m_h T}{m_c V_c}\right)^{1/2}\left(\sqrt{\frac{m_h}{m_c}\frac{|V_v|}{V_c}} + \frac{3V_c - |V_v|}{2V_c}\right)$$
$$+ \left(\frac{5V_c - |V_v|}{2V_c}\right)^2\frac{m_h}{m_c}\frac{T}{V_c}\right], \tag{46}$$

where $E_B = m_c e^4/2\hbar^2\kappa_0^2$ is the Bohr electron energy, n and p are the two-dimensional concentrations of the electrons and holes, respectively. The three terms in (42) are the result of the expansion of the matrix element in powers of $1/Q$. The g_1 and g_2 terms originate from the $M^{(1)}$ part of M, which corresponds to small momentum transfers during the Coulomb interactions of the electrons, and g_3 originates from the $M^{(2)}$ part of M, which corresponds to large momentum transfers.

5. RADIATIVE RECOMBINATION RATE

In order to analyze the lifetime of the nonequilibrium carriers in type-II heterostructures, as well as the internal quantum efficiency, we must calculate the radiative recombination rate, which is conveniently represented for two-dimensional carriers in the form[11]

$$R = \frac{np}{n_i^2} R_0,$$ (47)

where

$$R_0 = \frac{\varepsilon_\infty}{\pi^2 c^2} \int \frac{\alpha(\omega)\omega^2 d\omega}{\exp(\hbar\omega/T)-1},$$ (48)

$$n_i^2 \simeq 4\left(\frac{T}{2\pi\hbar^2}\right)^2 m_c m_h \exp\left(-\frac{\tilde{E}_g}{T}\right),$$ (49)

$$\alpha(\omega) = \frac{2\pi}{\hbar} \frac{1}{N_f} \sum_{c,v} |M_R|^2 \delta(E_c - E_v - \hbar\omega),$$ (50)

ω is the frequency of the photon emitted, ε_∞ is the high-frequency dielectric constant of the narrow-gap semiconductor, $\tilde{E}_g = E_g + E_{0c} + E_{0h}$, N_{ph} is the photon density, the subscripts c and v correspond to electron states in the conduction band and hole states in the valence band, and M_R is the optical transition matrix element. Using the explicit forms of the electron and hole wave functions, we represent the square of the absolute value of the matrix element in the form

$$|M_R|^2 = \frac{2\pi}{\sqrt{\kappa_0}} \frac{c^2}{\hbar c} \frac{\gamma^2}{\omega} N_f (\mathbf{P}\cdot\mathbf{e})^2 \delta_{\mathbf{q}_c,\mathbf{q}_v}.$$ (51)

Here $\mathbf{e}$ is the polarization unit vector, which is directed parallel to the electric field of the wave; we recall that $\mathbf{q}_{c,v}$ is the wave vector of the particles in the plane of the heterointerface;

$$\mathbf{P} = \frac{1}{i\gamma} \int \mathbf{j}_{cv}(x)dx \equiv (P_x, \mathbf{P}_\parallel).$$ (52)

The flux density $\mathbf{j}_{cv}$ is given by (19).

Substituting the explicit expressions for the components of the electron and hole wave functions (u and v) into (52) and performing the integration with respect to x, we obtain

$$P_x = iB\left\{ \frac{Hq_c}{\kappa_c^2 + p_h^2}\left[p_h \cos\frac{p_h b}{2} - \kappa_c \sin\frac{p_h b}{2}\right]\right.$$

$$+ \frac{Lp_l}{\kappa_c^2 + p_l^2}\left[p_l \cos\frac{p_l b}{2} - \kappa_c \sin\frac{p_l b}{2}\right]$$

$$\left. - \frac{\tilde{H}q_c}{\kappa_h^2 + k^2}(\kappa_h + \kappa_c) + \frac{\tilde{L}\kappa_l}{\kappa_l^2 + k^2}(\kappa_l + \kappa_c)\right\} \equiv P_x^E + p_x^H,$$ (53)

$$|\mathbf{P}_\parallel| = B\left\{ -\frac{Hp_h}{\kappa_c^2 + p_h^2}\left[\kappa_c \cos\frac{p_h b}{2} + p_h \sin\frac{p_h b}{2}\right]\right.$$

$$+ \frac{Lq_c}{\kappa_c^2 + p_l^2}\left[\kappa_c \cos\frac{p_l b}{2} + p_l \sin\frac{p_l b}{2}\right]$$

$$\left. + \frac{\tilde{H}\kappa_h}{\kappa_h^2 + k^2}(\kappa_h + \kappa_c) - \frac{\tilde{L}q_c}{\kappa_l^2 + k^2}(\kappa_l + \kappa_c)\right\} \equiv P_\parallel^E + P_\parallel^H.$$ (54)

Here $P_{x,\parallel}^E$ and $P_{x,\parallel}^H$ correspond to the two channels E and H for electron-hole recombination (see Fig. 2). The terms proportional to H and L in (53) and (54) correspond to $P_{x,\parallel}^E$, and the terms proportional to $\tilde{H}$ and $\tilde{L}$ correspond to $P_{x,\parallel}^H$. We recall that the E channel corresponds to the recombination of a tunneling electron with a hole in the quantum well and that the H channel corresponds to the recombination of a tunneling hole with an electron in the quantum well.

As we know, the contributions to the radiative recombination rate in the case of nondegenerate electron statistics are made by values of $q \leqslant q_T$, where $q_T = 1/\lambda_T$. It follows from (53) and (54) that we have $|P_x| \ll |\mathbf{P}_\parallel|$ when $q \leqslant q_T$:

$$\frac{|P_x|}{|\mathbf{P}_\parallel|} \approx \frac{m_c}{m_h} \sqrt{\frac{V_c}{|V_v|}} \ll 1.$$ (55)

Therefore, the main contribution to the radiative recombination rate is made by $\mathbf{P}_\parallel$. As follows from (53) and (54), when $q_c = q_v = 0$, we have $P_x = 0$, and $\mathbf{P}_\parallel$ is nonzero:

$$|\mathbf{P}_\parallel| \simeq HB \sin\left(\frac{p_h b}{2}\right) \frac{p_h^2}{\kappa_c^2 + p_h^2}.$$ (56)

Here we have taken into account that the holes are found in a size-quantization level of the heavy holes and $\kappa_c > p_h$. It is noteworthy that $\mathbf{P}_\parallel$ is weakly dependent on q_c and q_v. In addition, $\mathbf{P}_\parallel(q_c = q_v = 0) \approx \mathbf{P}_\parallel(q_c = q_v = q_T)$. Thus, the optical transition matrix element M_R is determined by $\mathbf{P}_\parallel$ and scarcely depends on q_c and q_v. Therefore, in the further calculations of the radiative recombination rate we can set $q_c = q_v = 0$ in the expression for $\mathbf{P}_\parallel$. We recall that the Auger transition matrix element is shortly dependent on the longitudinal components of the electron momentum (q_2) and the hole momentum (q_3) and that when $q_2 = q_3 = 0$ holds, the Auger transition matrix element equals zero [see Eqs. (16), (20), and (23)].

It should also be noted that the contributions of the two recombination channels (E and H) to $\mathbf{P}_\parallel$ differ significantly:

$$\frac{P_\parallel^H}{P_\parallel^E} \approx \frac{m_c}{m_h} \ll 1,$$ (57)

A conclusion of fundamental importance follows from (57): the optical transition matrix element M_R and, therefore, the radiative recombination rate in type-II heterostructures is determined by the E channel for electron-hole recombination. As was shown above, in the case of Auger recombination, the contributions of the E and H channels to the Auger transition matrix element are of the same order, but of different sign, and when they are summed, they compensate one an-

other. As a result, destructive interference of the E and H channels takes place for Auger recombination with a resultant decrease in its rate.

Some comments on the physical meaning of the interference mechanism of the two channels (E and H) in the Auger recombination rate and the predominance of the E channel over the H recombination channel in the case of radiative recombination are in order.

As we have already noted, the Auger recombination matrix element for small momentum transfers is proportional to the difference between the longitudinal components of the momenta of the electrons and holes $\mathbf{q}_3-\mathbf{q}_2=\mathbf{q}_1-\mathbf{q}_4$ [see Eqs. (16), (20), and (23)]. When $\mathbf{q}_3$ is nonzero, interconversion of the light and heavy holes occurs upon interaction with the heterointerface. As a result, a hole incident to the heterointerface tunnels through the heterobarrier with a light mass. This results in a significant increase in the part of the Auger recombination matrix element corresponding to the H channel, which is of the same order as the matrix element corresponding to the E channel, but of opposite sign.

Such destructive interference of the E and H channels does not occur for radiative recombination, since, as we have already noted, M_R is weakly dependent on the longitudinal momenta of the electrons (q_c) and holes (q_v). Also, since the mutual transformation of light and heavy holes does not take place at $q_v=0$, this process is not important for optical transitions. In this case the H channel of electron-hole recombination is ineffective, since it corresponds to the tunneling of a hole with a heavy mass. As a result, in the case of optical transitions, the ratio between $P_{\parallel}^H$ and $P_{\parallel}^E$ is given by (57).

Thus, for $|M_R|^2$ we obtain

$$|M_R|^2=\frac{2\pi}{\sqrt{\kappa_0}}\frac{e^2}{\hbar c}\frac{\gamma^2}{\omega}\,N_f(\mathbf{P}_{\parallel}\cdot\mathbf{e})^2\delta_{\mathbf{q}_c,\mathbf{q}_c},\tag{58}$$

We substitute (58) and (50) into (48). Performing the summation over the c and v states of the particles and integrating with respect to ω, for the radiative recombination rate we obtain

$$R\simeq\frac{\pi}{2}\frac{\varepsilon_\infty}{\sqrt{\kappa_0}}\frac{e^2}{\hbar c}\frac{E_g}{\hbar}\frac{E_g}{m_cc^2}\frac{\hbar^2np}{2m_cV_c}\frac{T}{V_c}\frac{m_h}{m_c}.\tag{59}$$

We note that the radiative recombination process of electrons and holes is just as effective in type-II heterostructures as in type-I heterostructures. For comparison we present the ratio of the radiative recombination rates $R\equiv R_{II}$ and R_I in type-II and type-I heterostructures, respectively, for the same heterostructure parameters:

$$R_{II}/R_I\simeq\left(\frac{Tm_h}{V_cm_c}\right)^2\leqslant 1.$$

6. DISCUSSION OF RESULTS

As follows from (42), the Auger recombination rate is a power function of the temperature. In addition, G is highly dependent on the parameters a, b, V_c, and V_v of the heterostructure.

As we have already noted, G_1 and G_2 in (42) originate from the part $M^{(1)}$ of the matrix element M, which corresponds to small momentum transfers in the Coulomb interaction of the electrons, while G_3 originates from the part $M^{(2)}$ of M, which corresponds to large momentum transfers. We note that, as follows from (42)–(46), when $V_c>|V_v|$ holds, we have $G_1>G_2\gg G_3$. It should be specially stressed that under the condition $3V_c\approx|V_v|$, i.e., $(3V_c-|V_v|)/V_c\ll1$, we have $G_1\ll(G_2,G_3)$. Under another condition $3V_c\approx|V_v|$ we have $G_2\ll(G_1,G_3)$. This means that G_1 and G_2 have a minimum at the values of $|V_v|/V_c$ just indicated (Fig. 4). Therefore, the Auger recombination rate has a minimum at certain values of $|V_v|/V_c$: $G^{min}\approx G_3$. Thus, the minimal value of the Auger recombination rate G^{min} is determined by the Coulomb interaction matrix element $M^{(2)}$ for large momentum transfers. This means that there is effective suppression of the Auger recombination processes in Type-II heterostructures, since, as we have already noted, when $V_c>|V_v|,G_3\ll(G_1,G_2)$.

Such effective suppression of the Auger recombination rate in type-II heterostructures is attributed to the behavior of the overlap integral $I_{14}(q)$ of the electron in the initial state 1 and the final state 4 for a small momentum transfer q. This overlap integral has contributions from three regions: the two regions for subbarrier motion of the electron ($x<-a$ and $x>0$) and the region of the quantum well ($-a<x<0$). When the contributions from these three regions are summed, it is found in the case of both type-I and type-II heterostructures that the contributions from the subbarrier regions and the region of the quantum well cancel. The resultant overlap integral is diminished by a factor of $(3V_c+V_v)/E_g$. We note that for type-I heterostructures $V_v>0$ and that for type-II heterostructures $V_v=-|V_v|<0$. Consequently, we find that in type-II heterostructures there is a strong decrease in the overlap integral $I_{14}(q)$ of the electron in the initial and final states when the momentum transfer q is small under the condition $3V_c\simeq|V_v|$. This is a result of the cancellation of the contributions to $I_{14}(q)$ of the regions indicated above.

Figure 4 presents the dependence of the logarithm of the Auger recombination rate on the ratio $|V_v|/V_c$ calculated from (42) with consideration of the exact expressions for g_1, g_2, and g_3 [see (43)–(46)]. We obtained a result of fundamental importance: the Auger recombination rate has a minimum for $3V_c\simeq|V_v|$. Also, the ratio of the Auger recombination rate $G^{min}\equiv G(3V_c\sim|V_v|)$ at the minimum to the rate for $V_c\geqslant|V_v|$ is small: $G^{min}/G(V_c\geqslant|V_v|)\ll1$. The result obtained is of fundamental importance, since it demonstrates the possibility of suppressing the Auger recombination processes in type-II heterostructures. Such effective suppression of these processes is attributed to the nature of the Coulomb interaction between the electrons in an Auger transition. Under some conditions ($|V_v|<V_c$) the Coulomb interaction between the electrons is mainly an effective long-range interaction (small momentum transfers), producing a large value for the Auger recombination rate. Under other conditions ($3V_c\approx|V_v|$) the Coulomb interaction between the electrons has a predominantly short-range character (large momentum
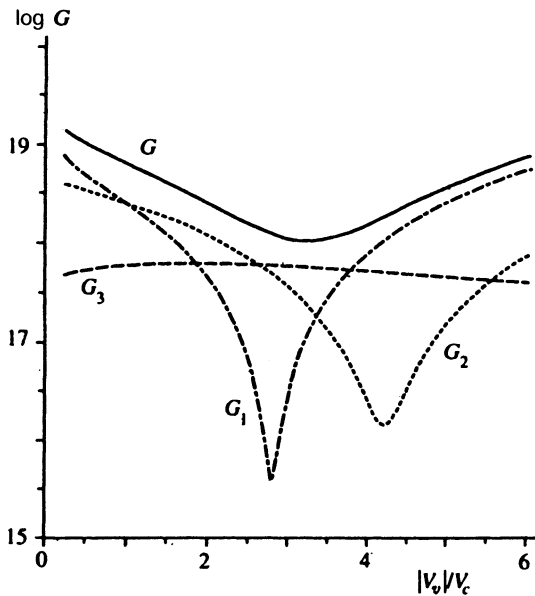
FIG. 4. Logarithm of the Auger recombination rate $\log G$ versus $|V_v|/V_c$ at $T=290$ K. The dashed curves correspond to the contributions G_1, G_2, and G_3 to G. The solid curve corresponds to the total rate G. The following parameters, which are characteristic of an InP/AlInAs structure,[4] were used in the calculation: $E_g=0.96$ eV, $V_c=0.15$ eV, $m_c=0.05m_0$, $m_h=0.4m_0$, $a=b=80$ Å, $n=p=1.2\times10^{12}$ cm^{-2}.
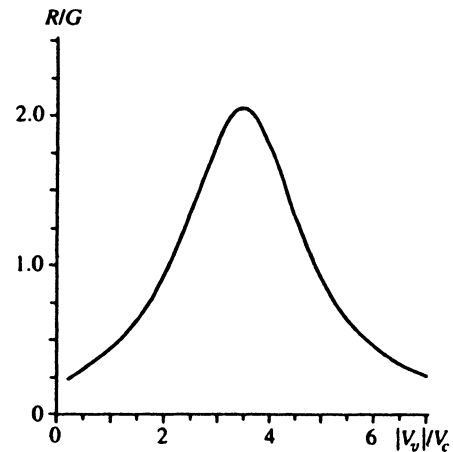

FIG. 5. Dependence of the ratio between the radiative (R) and Auger (G) recombination rates on $|V_v|/V_c$ at $T=290$ K. The following parameters, which are characteristic of an InGaAsSb/GaSb structure,[4] were used in the calculation: $E_g=0.6$ eV, $V_c=0.25$ eV, $m_c=0.04m_0$, $m_h=0.4m_0$, $a=b=100$ Å, $n=p=7\times10^{11}$ cm^{-2}.

transfers), causing a sharp decrease in the Auger recombination rate.

Suppression of the Auger recombination process in type-II heterostructures is of fundamental importance for creating optoelectronic devices with improved characteristics. Auger recombination processes are known to cause a decrease in the internal quantum efficiency of semiconductor quantum-well lasers and an increase in the threshold current density at high temperatures.[12] The mechanism for suppressing Auger recombination processes in type-II heterostructures predicted in the present work makes it possible, in particular, to solve the problem of long-wavelength lasers ($\lambda>4$ mμ), viz., to raise their working temperature to room and higher temperatures.

It is interesting to compare the Auger recombination rate in type-II heterostructures at the minimum with the rate in type-I heterostructures G_I. Using the expression for G_I from Ref. 12, for equal values of the heterostructure parameters we have

$$\frac{G^{min}}{G_I} \sim \left(\frac{T}{V_c}\frac{m_h}{m_c}\right)^3 \frac{V_c}{E_g} \ll 1. \tag{60}$$

Therefore, in type-II heterostructures, unlike type-I heterostructures, a significant decrease in the rate of the Auger recombination processes is possible. This conclusion, in particular, can be significant in developing optoelectronic devices.

Let us proceed to an analysis of the radiative recombination rate in type-II heterostructures. As has already been noted, the radiative recombination rates in type-II ($R \equiv R_{II}$) and type-I (R_I) heterostructures are of the same order: $R_{II} \leqslant R_I$.

In the case of quantum wells based on narrow-gap semiconductors,[12] the Auger recombination rate in type-I heterostructures (G_I) is known to significantly exceed the radiative recombination rate (R_I) at high temperatures. Therefore, in these semiconductor structures the internal quantum efficiency η is much less than unity: $\eta = R_I/(G_I+R_I) \ll 1$.

In type-II heterostructures the situation can be the exact opposite. The ratio between the radiative and Auger recombination rates in these heterostructures has a sharp maximum as a function of $|V_v|/V_c$ (Fig. 5). It is noteworthy that for type-II heterostructures even with a small value for the effective band gap width E_g the value of R_{II}/G_{II} at the maximum can be greater than unity. Consequently, by selecting the optimal parameters for the heterostructure (at which R/G is a maximum), we can achieve the maximum internal quantum efficiency η for long-wavelength lasers based on type-II heterostructures.

The mechanism for suppressing the Auger recombination processes that was theoretically predicted in the present work was detected experimentally when a laser of a new type employing a single InAs/GaSb type-II heterojunction was created.[13] Suppression of the Auger recombination processes in type-II heterostructures with a superlattice based on In(As, Sb) was also discovered in another experimental study.[14]

7. CONCLUSIONS

We summarize the main results of this work.

1) It has been shown that the Auger-recombination process is always a threshold-free process in type-II heterostructures and that its rate is a power function of the temperature.

2) The fundamental difference between the mechanisms of the Auger recombination of nonequilibrium carriers in type-I and type-II heterostructures has been demonstrated:

a) in type-II heterostructures there are two channels for Auger recombination, viz., E and H, which interfere with one another to a significant degree;

b) G_{II} and G_I depend on the heterostructure parameters V_c and V_v significantly different: G_{II} has a minimum as a function of $|V_v|/V_c$, while G_I is an increasing function of V_v/V_c;

c) the Auger recombination rate is suppressed in type-II heterostructures in comparison with type-I heterostructures;

d) in quantum wells for which $E_{0h}<T<E_{0c}$ holds the temperature dependence of G_{II} differs from that of G_I: $G_{II}\propto T^2$ and $G_I\propto 1/T$. It follows from this analysis that in the temperature range where the recombination of nonequilibrium carriers is determined by the nonradiative channel, the lifetime $\tau=n/G$ is greater in type-II structures than in type-I structures.

3) Another fundamental conclusion of the present work is as follows: the radiative recombination rate in type-II heterostructures is of the same order as in type-I heterostructures with the same parameters.

4) It has been shown that in type-II heterostructures the internal quantum efficiency η can be significantly higher than the quantum efficiency in type-I structures with the same parameters.

5) We predict a significant decrease in the value of the threshold current density of lasers based on type-II heterostructures in comparison with lasers based on type-I heterostructures owing to the mechanism for suppressing the Auger recombination rate when the ratio of the barrier heights V_v and $V_c(3|V_v|\simeq V_c)$ has a certain value. We shall not analyze the influence of the recombination processes studied on the operation of optoelectronic devices in detail here. The purpose of the present study was to investigate the mechanisms of radiative and Auger recombination in type-II heterostructures and to ascertain the main features distinguishing them from the recombination mechanisms in type-I heterostructures.

APPENDIX: A

Using the boundary conditions (4) and the explicit form of the wave functions for holes [Eqs. (8) and (9)], we express the amplitudes $\tilde{H}$, $\tilde{L}$, and L in terms of the amplitude H of a heavy hole in the well:

$$\tilde{H}=-\frac{\varepsilon_h}{|V_v|}H\sin\frac{p_h b}{2}, \tag{A1}$$

$$\tilde{L}=\frac{\varepsilon_h}{|V_v|}\frac{q_3}{|p_l|}H\sin\frac{p_h b}{2}, \tag{A2}$$

$$L=H\frac{\sin(p_h b/2)}{\sin(p_l b/2)}\left[\frac{q_3}{|p_l|}\left(l+\frac{\varepsilon_h}{|V_v|}\right)+\frac{q_3}{|p_l|^2}\sqrt{\frac{2m_c\varepsilon_h^2}{\hbar^2|V_v|}}\right.$$
$$\left.+\frac{q_3}{|p_l|^3}\frac{2m_c\varepsilon_h^2}{\hbar^2|V_v|}\right]. \tag{A3}$$

The expressions (A1)–(A3) were written for states for which the component v_{3x} is an odd function relative to the middle of the well for holes $x=b/2$. There is an analogous expression for the states of the other parity. In deriving (A1)–(A3) we took into account that $\varepsilon_h\ll|V_v|$. The amplitude H of a heavy hole in the quantum well is calculated from the normalization condition for the wave function and has the form

$$H=\sqrt{\frac{2}{b(p_h^2+q_3^2)}}. \tag{A4}$$

Note that in the interesting range of values $q_3>1/b$ the x component of the wave vector of a light hole p_l in the region of the well is purely imaginary: $p_l\equiv i|p_l|$, where $|p_l|\approx q_3$.

Using the explicit form of the wave functions of the highly excited electron (11)–(13) and the boundary conditions (3), for the amplitudes r, d_+, d_-, and t we obtain

$$t=e^{i\varphi}, \quad d_+=e^{l\varphi}(1-\delta), \quad d_-=\delta e^{i\varphi},$$

$$r=2i\,\delta e^{i\varphi}\sin k_4 a, \quad \varphi=a(k_4-\bar{k}_4), \quad \delta=\frac{2V_c-|V_v|}{8E_g}\ll 1. \tag{A5}$$

In (A5) we took into account the explicit form of A_4. The expressions (A5) were written for the case of $\delta\ll 1$.

APPENDIX: B

We substitute the explicit expressions for the wave functions of electrons in states 1 and 4 from (5), (6), and (11)–(13) into (22). Performing the integration with respect to x, we obtain the expression for I_x:

$$I_x=A_4Be^{-iqa}\left\{i\lambda_+^{(1)}\kappa_c\left[\frac{\exp(-\bar{k}_q a)}{\kappa_c+iq+i\bar{k}_4}+\frac{r\exp(\bar{k}_4 a)}{\kappa_c+iq-i\bar{k}_4}\right]\right.$$

$$\left.+\lambda_+^{(4)}\bar{k}_4\left[\frac{\exp(-\bar{k}_4 a)}{\kappa_c+iq+i\bar{k}_4}-\frac{r\exp(\bar{k}_4 a)}{\kappa_c+iq-i\bar{k}_4}\right]\right\}$$

$$+\frac{AA_4}{2i}\sum_{\nu=-1,1}[\lambda_-^{(4)}k_4-\nu\lambda_-^{(1)}k]$$

$$\times\left[d_+\frac{\exp(i\nu ka/2)-\exp[-i(q+k_4)a-i\nu ka/2]}{q+\nu k+k_4}\right.$$

$$\left.-d_-\frac{\exp(-i\nu ka/2)-\exp(-i(q-k_4)a+i\nu ka/2)}{q-\nu k-k_4}\right]$$

$$+\frac{A_4 tB}{\kappa_c-iq-\bar{k}_4}\{\lambda_+^{(4)}\bar{k}_4-i\lambda_+^{(1)}\kappa_c\}. \tag{B1}$$

It follows from (B1) that the integration of I_x with respect to q in the plane of the complex variable q produces poles at the points $q=\bar{k}_4\pm i\kappa_c$ and $q=k_4\pm k$. These poles in

I_x correspond to large momentum transfers $q \approx Q$, since $k_4 \approx \bar{k}_4 \approx Q \gg (k, \kappa_c)$. We note that the expression for $\mathbf{I}_\parallel$ can be calculated using (21) and the explicit forms of the wave functions (5), (6), and (11)–(13). The final expression for $I_\parallel$ has a form similar to (B1); the dependence of $\mathbf{I}_\parallel$ on q is the same as that of I_x. It is also significant that the poles of $\mathbf{I}_\parallel$ and I_x appearing in the q plane as a result of the integration with respect to q coincide.

APPENDIX: C

According to (33), the expression for $J_{14}^{(e)}$ has the form

$$J_{14}^{(e)} = \int_{-\infty}^{0} \frac{dq}{2\pi} I_{14}(q) \frac{e^{-iqx}}{q^2 + p_{14}^2}. \tag{C1}$$

Integrating with respect to q in (C1) with the aid of the residue theorem and discarding the poles corresponding to small momentum transfers at $q = \pm i p_{14}$, which were already taken in $M^{(1)}$, we obtain the following expression for $J_{14}^{(e)}$:

$$J_{14}^{(e)} = \frac{A_4 A}{2} \sum_{\nu=-1,1} \frac{d_+ \exp[il(\nu)] + d_- \exp[-il(\nu)]}{p_{14}^2 + (Q + \nu k)^2}$$

$$\times [1 + \lambda_-^{(1)} \lambda_-^{(4)} (\mathbf{q}_1 \mathbf{q}_4 - \nu k k_4)]. \tag{C2}$$

where $l(\nu) = \nu k x_a + \kappa_4 x$.

[1] *Quantum Well Lasers*, edited by P. S. Zory, Academic Press, New York, 1993.

[2] É. I. Rashba and V. B. Timofeev, Fiz. Tekh. Poluprovodn. **20**, 977 (1986) [Sov. Phys. Semicond. **20**, 617 (1986)].

[3] G. G. Zegrya and V. A. Kharchenko, Zh. Eksp. Teor. Fiz. **101**, 327 (1992) [Sov. Phys. JETP **74**, 173 (1992)].

[4] M. P. Mikhailova and A. N. Titkov, Semicond. Sci. Technol. **9**, 1279 (1994).

[5] B. L. Gel'mont, Zh. Eksp. Teor. Fiz. **75**, 536 (1978) [Sov. Phys. JETP **48**, 268 (1978)].

[6] E. O. Kane, J. Phys. Chem. Solids **1**, 249 (1957).

[7] A. V. Sokol'skiĭ and R. A. Suris, Fiz. Tekh. Poluprovodn. **21**, 866 (1987) [Sov. Phys. Semicond. **21**, 529 (1987)].

[8] L. D. Landau and E. M. Lifshitz, *Quantum Mechanics: Non-Relativistic Theory*, 3rd. edn., Pergamon Press, Oxford, 1977.

[9] V. I. Smirnov, *A Course of Higher Mathematics*, Vol. 3, Addison-Wesley, Reading, MA (Fig. 4).

[10] M. I. Dyakonov and V. Yu. Kachorovskii, Phys. Rev. B **49**, 17 130 (1994).

[11] B. L. Gel'mont and G. G. Zegrya, Fiz. Tekh. Poluprovodn. **25**, 2019 (1991) [Sov. Phys. Semicond. **25**, 1216 (1991)].

[12] G. G. Zegrya, A. D. Andreev, N. A. Gun'ko, and E. V. Frolushkina, Proc. Soc. Photo-Opt. Instrum. Eng. **2399**, 307 (1995).

[13] M. P. Mikhailova, G. G. Zegrya, K. D. Molseev, *et al.*, Proc. Soc. Photo-Opt. Instrum. Eng. **2397**, 166 (1995).

[14] P. J. P. Tang, M. J. Pullin, S. J. Chung, *et al.*, Proc. Soc. Photo-Opt. Instrum. Eng. **2397**, 389 (1995).

Translated by P. Shelnitz